

Realistic inversion of diffraction data for an amorphous solid: The case of amorphous siliconAnup Pandey,^{1,*} Parthapratim Biswas,^{2,†} Bishal Bhattarai,^{1,‡} and D. A. Drabold^{3,§}¹*Department of Physics and Astronomy, Condensed Matter and Surface Science Program, Ohio University, Athens, Ohio 45701, USA*²*Department of Physics and Astronomy, The University of Southern Mississippi, Hattiesburg, Mississippi 39406, USA*³*Department of Physics and Astronomy, Nanoscale and Quantum Phenomena Institute, Ohio University, Athens, Ohio 45701, USA*

(Received 27 September 2016; revised manuscript received 4 December 2016; published 22 December 2016)

We apply a method called “force-enhanced atomic refinement” (FEAR) to create a computer model of amorphous silicon (*a*-Si) based upon the highly precise x-ray diffraction experiments of Laaziri *et al.* [*Phys. Rev. Lett.* **82**, 3460 (1999)]. The logic underlying our calculation is to estimate the structure of a real sample *a*-Si using experimental data and chemical information included in a nonbiased way, starting from random coordinates. The model is in close agreement with experiment *and* also sits at a suitable energy minimum according to density-functional calculations. In agreement with experiments, we find a small concentration of coordination defects that we discuss, including their electronic consequences. The gap states in the FEAR model are delocalized compared to a continuous random network model. The method is more efficient and accurate, in the sense of fitting the diffraction data, than conventional melt-quench methods. We compute the vibrational density of states and the specific heat, and we find that both compare favorably to experiments.

DOI: [10.1103/PhysRevB.94.235208](https://doi.org/10.1103/PhysRevB.94.235208)**I. INTRODUCTION**

It has long been realized that the inversion of diffraction data—extracting a structural model based upon the data at hand—is a difficult problem of materials theory. It is worth noting that the success of inverting diffraction data for crystals has been one of the profound success stories of science, even revealing the structure of the ribosome [1]. The situation is different for noncrystalline materials. Evidence from reverse Monte Carlo (RMC) studies [2–5] shows that the information inherent to pair correlations alone is not adequate to produce a model with chemically realistic coordination and ordering. This is not really surprising, as the structure factor $S(Q)$ or pair-correlation function $g(r)$ (PCF) is a smooth one-dimensional function, and its information entropy [6] is vastly higher (and its information commensurately lower) than for a crystal, the latter PCF being a sequence of sharply localized functions. It seems clear that including chemical information, *in an unbiased mode*, should aid the structure determination substantially. Others have clearly described this challenge as the “nanostructure problem” [7], and the appeal of including an interatomic potential has been noted. We show here that such an approach is successful by uniting the RMC code RMCPROFILE and including chemistry in a self-consistent manner using density-functional theory, but not by invoking *ad hoc* constraints. We have named this method “force-enhanced atomic refinement” (FEAR). In this paper, we focus on the classic and persistently vexing problem of amorphous silicon. The details of the methods can be found elsewhere [8,9]. The method is fast enough to make it easy to implement with *ab initio* interactions (SIESTA here) and plane-wave DFT (VASP) as we used in ternary chalcogenide materials in Ref. [9].

The technological importance of *a*-Si in microelectronics, thin-film transistors, and photovoltaic (PV) applications [10] has led to many studies in recent decades [11–16]. In addition, the overconstrained network makes the structure of *a*-Si difficult to model [17,18]. The only method that produces really satisfactory models for *a*-Si is the Wooten-Weaire-Winer (WWW) [18] scheme, which is limited by unrealistic interactions and is also not a general technique.

From a practical modeling perspective, the utilization of *a priori* information by constraining chemical order and preferred coordination has improved some of the most serious limitations of RMC [2,19]. Cliffe and co-workers imposed “uniformity” as a constraint in a refinement of atomistic-scale structures in their invariant environment refinement technique (INVERT) [20], and they extended their analysis considerably by invoking “structural simplicity” as a guiding principle in modeling *a*-Si [21]. Recently, another angle has been tried: including electronic *a priori* information in the form of an imposed band gap [22,23]. These constraints are externally imposed, and although they are sensible, they introduce investigator *bias* in the modeling. In other applications, more along the lines of “materials by design,” the point is indeed to impose conditions that the model must obey, and to see if a physical realization of the desired properties may be realized. This is beyond the scope of the present paper, which is focused on trying to best understand well-explored specific samples of *a*-Si.

More in the spirit of our work, a hybrid reverse Monte Carlo (HRMC) incorporating experimental data and a penalty function scheme was introduced to find models of amorphous carbon in agreement with diffraction data also near a minimum of an empirical potential [24]. Gereben and Pusztai employed a similar approach of hybrid RMC with bonded and nonbonded forces to study liquid dimethyl trisulfide [25]. A method known as empirical potential structure refinement (EPSR) has been successful in modeling amorphous and liquid structures by refining the initial interatomic empirical potential energy function while fitting the structure factor data [26]. The first attempt to incorporate experimental information

*ap43911@ohio.edu

†partha.biswas@usm.edu

‡bb248213@ohio.edu

§drabold@ohio.edu

in a first-principle approach was experimentally constrained molecular relaxation (ECMR) [27,28]. ECMR merely alternated full relaxations of fitting pair correlations (via RMC) and energy minimization. When this process converged (as it did for the case of glassy GeSe₂), an excellent model resulted [27]. The problem was that this scheme often failed to converge. We therefore amended ECMR and introduced *ab initio* force-enhanced atomic refinement (*ab initio* FEAR) [9]. In effect, we alternate between partially fitting the RDF (or structure factor) using RMC and carrying out partial relaxations using *ab initio* interactions, as we explain in detail in Refs. [8,9]. By carrying out the iteration in “bite-sized” bits rather than iterated full relaxations, as in the original ECMR, we find that the method is robust, working for silver-doped chalcogenides with plane-wave DFT and for WWW *a*-Si with SIESTA and also for forms of amorphous carbon [29].

We should clarify that in our previous work on *a*-Si [9], we used the WWW pair-correlation data as input “experimental data,” whereas in this work we have used high-energy x-ray diffraction data from Laaziri *et al.* [14]. WWW models are a fixture of the modeling community (a continuous random network of ideal fourfold coordination and involving up to 100 000 atoms [13,30]), and they represent an important benchmark that a new method must handle. It is reasonably interpreted as “ideal” *a*-Si, with minimum strain. While the pair-correlation data of WWW and Laaziri [14] are indeed fairly similar, there are key differences, as noted by Roorda and co-workers [16]. Given the high quality and precision of the experiments, we have undertaken a FEAR inversion of their data in this paper.

One key assumption that we emphasize forthrightly is that the dataset of Laaziri and co-workers may be represented by a small supercell model of silicon. This is obviously an approximation, as the material must surely include some voids and damaged regions from the ion bombardment procedure from which the material was made, and of course the x-ray diffraction includes these. While we think this is a reasonable approximation, it is clear that a very large-scale simulation with thousands of atoms allowing for internal surfaces and other inhomogeneities would be desirable, perhaps opening up the possibility of paracrystallites [31] and other longer length scale irregularities. While it is not obvious whether the RDF by itself would provide enough information to open up voids, recent studies on hydrogenated *a*-Si have demonstrated that inversion of experimental nuclear magnetic resonance (NMR) [32,33] and infrared (IR) data [34,35] can produce, in association with *ab initio* interactions, nanoscale inhomogeneities, such as voids and extended defect structures in *a*-Si:H. Further progress in this direction might be undertaken with transferable potentials devised from “machine learning” algorithms [36].

In our applications of FEAR, we have always started with a *random* model, and even for a complex ternary [9] the method converges with satisfactory and chemically sensible results. In effect, chemical information is provided through the partial CG relaxations, and the method explores the configuration space rather well, thanks to the excellent RMCPROFILE code [37].

The rest of this paper is organized as follows. In Sec. II, we summarize FEAR and describe the methodology for the

current work. In Sec. III, we present the results for a 216-atom *a*-Si FEAR model. The conclusions are given in Sec. IV.

II. METHODOLOGY

A detailed description of the FEAR method can be found elsewhere [8,9]. To summarize, in FEAR, a *random* starting configuration is subjected to partial RMC refinement followed by partial conjugate-gradient (CG) relaxations using a chemically realistic total-energy functional, e.g., *ab initio* interactions from density-functional theory. The two steps are repeated one after another until both the structure and energy converge to a prescribed accuracy [8,9]. A single FEAR step comprises M accepted RMC moves followed by N CG steps, and we denote the entire process by (M, N) . In this work, we have carried out a (500,5) process. Other combinations, such as $(M, N) = (1000, 5)/(1000, 20)/(6000, 5)$, are also explored, which, more or less, produce similar results but exhibit different convergence behavior. An (M, N) process is then repeated until convergence (namely finding a configuration that matches diffraction data and simultaneously being at a minimum of a DFT total-energy functional) is achieved. The RMC algorithm (in our case RMCPROFILE [37]) is used to invert the experimental data. We have so far only used diffraction data, but other experimental data, such as those from extended x-ray-absorption fine-structure (EXAFS) and NMR experiments, can also be used profitably as natural datasets. For complex materials, the use of multiple experimental datasets might be particularly beneficial to limit the number of unphysical configurations, while the CG relaxations enforce the local chemistry in the material. We employ a local-orbital basis DFT code (SIESTA) [38] using the local-density approximation (LDA). The cubic simulation cell (with 216 Si atoms) has a length of 16.28 Å, which corresponds to the experimental density of 2.33 gm cm⁻³ for *a*-Si. In the spirit of full reporting, this should be understood to be another *assumption*, which can be easily rectified by conducting a variable-cell CG optimization.

To illustrate the choice of the number of accepted RMC moves (M) and the number of CG steps (N) on the convergence of the structure, we have explored various combinations of (M, N) . While a small value of N (CG steps) is highly desirable from the viewpoint of computational cost, a very small N and large M (RMC steps) may not be able to steer the system to the correct solution space. Likewise, a very small value of M might not be enough to navigate the system out from a poor local minimum on the energy surface. To address this, we have studied the evolution of the number of fourfold-coordinated Si atoms in FEAR with a few combinations of M and N . A realistic model of *a*-Si must contain a higher percentage of fourfold silicon with fewer defects. The convergence for three different (M, N) processes is shown in Fig. 1. The structure is abruptly trapped into a local minimum for a higher value of CG steps ($N = 20$). The higher number of accepted RMC moves ($M = 6000$) generates a structure with a large density of coordination defects, which take a considerable number of FEAR steps to eliminate. For efficient use of the algorithm, we suggest an optimum value for M as anything between 100 and 2000 and for N any value between 3 and 20. Lower values

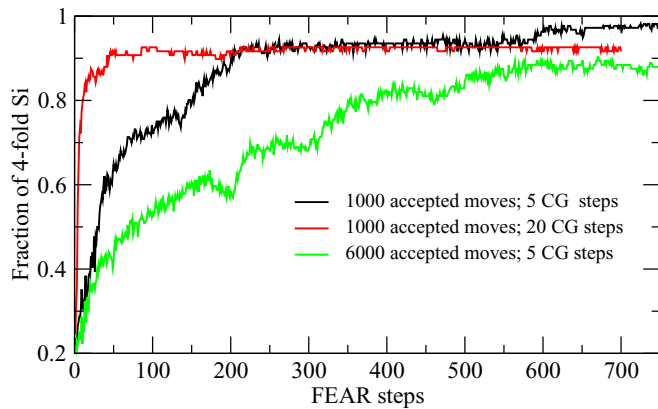


FIG. 1. The evolution of fourfold Si atoms during FEAR simulation for three different combinations of the number of accepted moves (M) and the number of CG steps (N). Black, $M = 1000$ and $N = 5$; red, $M = 1000$ and $N = 20$; and green, $M = 6000$ and $N = 5$.

of M and N make the method less expensive. Although there is no significant change in the structure by choice within this range, a short quick run with the extreme values is helpful to determine an appropriate value of M and N for new systems.

III. RESULTS AND DISCUSSION

In this section, we present results for a -Si obtained from FEAR. Since the method essentially consists of incorporating the pair-correlation data via reverse Monte Carlo simulations (RMC), followed by *ab initio* total-energy relaxations using the conjugate-gradient (CG) method, we also include the results from a CG-only model (obtained from the initial random state) to evaluate the performance of the FEAR method in relation to the CG-only relaxation as a function of simulation “time” or steps. In particular, we address the structure factor $S(Q)$, the bond-angle distribution $P(\theta)$, the electronic density of states (EDOS), the vibrational density of states (VDOS), and the vibrational specific heat from the FEAR model of a -Si. To examine the convergence of the method with respect to the total energy and the evolution of structure, we take a close look at the variation of the average coordination number and electronic gap as a function of FEAR steps.

Figure 2 shows the static structure factor of a -Si for the model configurations obtained from FEAR along with the structure-factor data of a -Si (annealed sample) reported by Lazirri *et al.* [14]. The results from the CG-only model are also included in Fig. 2 for comparison. Data fitting was carried out in Q space. We can see that the structure factor from the FEAR model compares very well with the experimental data. The only exceptions are a minor deviation of $S(Q)$ near $Q = 2.5$ and 7 \AA^{-1} . A comparison of the $S(Q)$ data from the FEAR and CG-only models suggests that the former is superior to the latter as far as the two-body correlations between atoms are concerned, even though both systems have been treated with identical *ab initio* DFT interactions. This observation is also reflected in Fig. 3, where the reduced radial distribution function, $G(r) = 4\pi r n_0 [g(r) - 1]$, obtained from FEAR, WWW, and x-ray-diffraction experiments, is plotted.

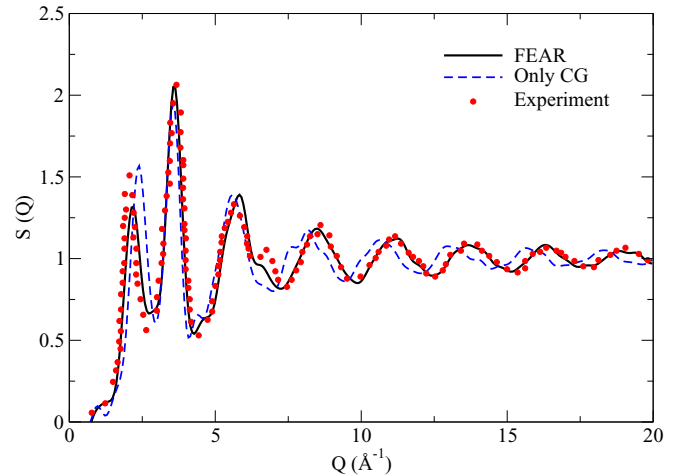


FIG. 2. Comparison of the simulated x-ray static structure factor from FEAR (black), CG-only (blue), and the experimental diffraction data (red circle) from Ref. [14]. A 216-atom model is used to compute the simulated structure factor.

Since the pair-correlation function or structure factor of a model cannot determine a three-dimensional amorphous structure uniquely, it is necessary to examine the models further by going beyond two-body correlation functions. Toward that end, we have calculated the bond-angle distribution $P(\theta)$, and we compared it with the results obtained from the WWW and CG-only models. Further, following Beeman *et al.* [17], we may assume that the half-width at half-maximum (HWHM) of the Raman TO peak of a -Si is related to the average width of the bond-angle distribution. Since a typical value of the full width of the Raman TO peak in a -Si ranges from 30 to 45 cm^{-1} , this approximately translates into a range of 12° – 17° for the RMS bond-angle deviation [39]. The value of the RMS bond-angle deviation (15.6°) obtained from the FEAR model is well within

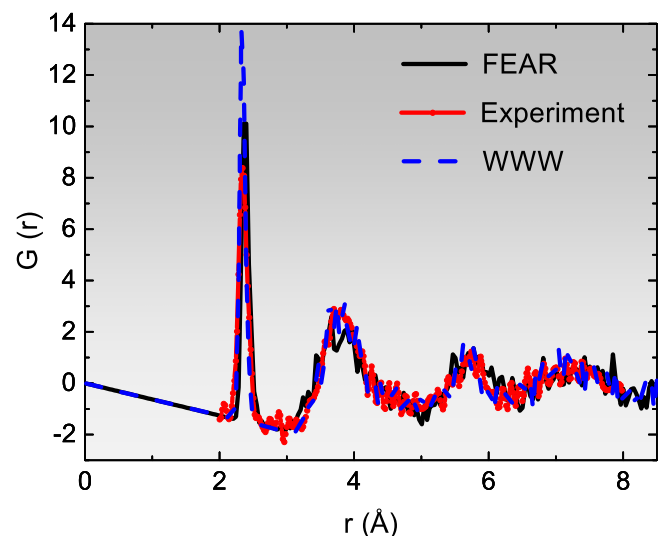


FIG. 3. The reduced pair-correlation function of a -Si obtained from a 216-atom model using the FEAR (black) and WWW (blue) methods. The experimental data (red) shown above are the Fourier transform of the high-energy x-ray diffraction data from Ref. [14].

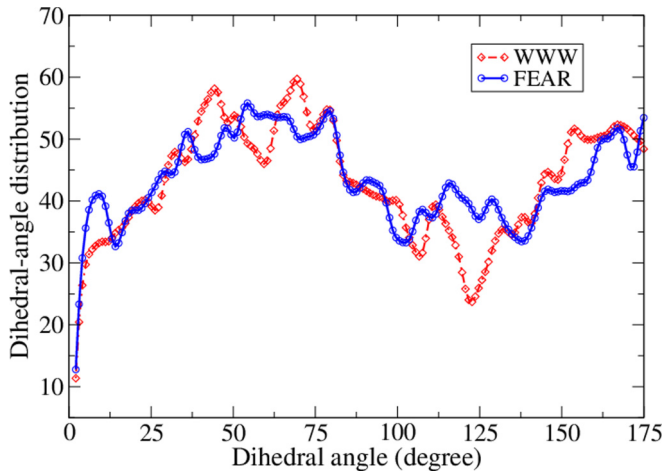


FIG. 4. Dihedral-angle distributions for two models of a -Si obtained from WWW and FEAR simulations, as indicated. For visual clarity, we have plotted a running average of the raw data, which slightly affects the distributions of very small and large angles.

the range of 12° – 17° . It is noteworthy that the FEAR model is statistically free of very small ($\leq 60^\circ$) or large ($\geq 160^\circ$) angles, and that the bond-angle distribution closely matches that from the WWW model. In contrast, a considerable number of small and large angles, below 60° and above 160° , respectively, have appeared in the bond-angle distribution of the CG-only and RMC-only models [9]. Thus, the FEAR method not only produces correct two-body correlations between atoms, but also a better *reduced* three-body correlations by judicious use of the input experimental data and the local chemical information of a -Si provided by the *ab initio* total-energy functional from SIESTA within the CG loop of the refinement process.

While structural information beyond three-body correlations proves to be highly nontrivial to obtain and analyze, it is possible to gather some information by looking at the dihedral-angle distribution involving four neighboring atoms and the ring statistics reflecting the topological connectivity of an amorphous network. Figure 4 presents the dihedral-angle distributions for a 216-atom FEAR model and a WWW model. Both distributions exhibit a maximum value near the dihedral angle of 60° and a minimum value in the vicinity of 120° . A minor deviation of the minimum in the FEAR model near 120° is probably indicative of slightly different dihedral correlations involving a chain of four neighboring atoms in the WWW and

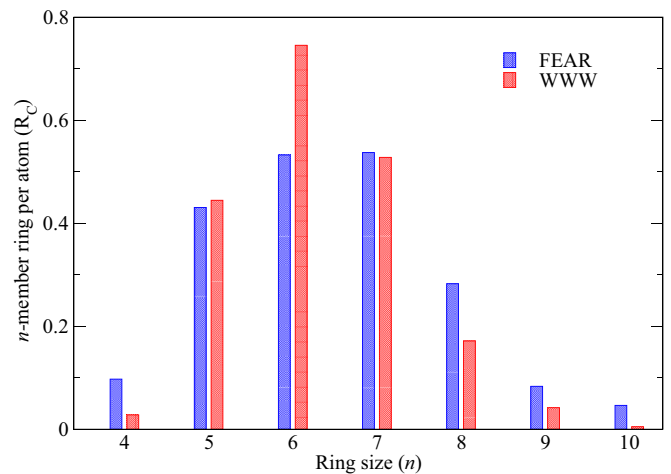


FIG. 5. The number of n -fold rings per atom (R_C) for the FEAR model (blue) compared to the WWW model of the same size.

FEAR models. We will see that such a deviation also affects the number of four-member rings in the FEAR models.

The ring statistics for the FEAR and WWW models are presented in Fig. 5. It is remarkable that the three-member rings are not present at all in the FEAR model, which is consistent with the absence of unphysical Si triangles in good-quality a -Si models. The only notable difference between the WWW model and the FEAR model is the existence of fewer six-member and more four-member rings in the latter. In Table I, we have listed the characteristic structural properties of the models along with the total energy per atom obtained from the density-functional code SIESTA. The FEAR model has 96% fourfold-coordinated atoms, with the remaining 4% being equally distributed between threefold- and fivefold-coordinated atoms. These values are equal to those obtained from the melt-quench model using environment-dependent interaction potential (96%) [40] and better than those obtained from other models in the literature [2,20,41]. The average coordination number of the FEAR model is found to be 4, which deviates from that of the experimental annealed sample (3.88) by Laaziri *et al.* [14] For comparison, we have presented the average coordination for various models in Table I using a nearest-neighbor distance of 2.75 \AA . It appears that the models with fewer coordination defects have higher average coordination than the experimentally reported value.

The variation of the total energy (E) and χ^2 with the number of FEAR steps is plotted in Fig. 6. The results suggest that the initial structure formation takes place very rapidly in

TABLE I. Total energy and key structural properties of a -Si models. The energy per atom is expressed with reference to the energy of the WWW model.

	RMC	CG	FEAR	WWW
Fourfold Si (%)	27	75	96	100
Threefold Si (%)	15	21	2	0
Fivefold Si (%)	25	3	2	0
Energy (eV/at)	3.84	0.09	0.06	0.00
Average bond angle (RMS deviation)	101.57° (31.12°)	107.31° (20.42°)	108.52° (15.59°)	108.97° (11.93°)
Average coordination number	4.27	3.83	4.00	4.00

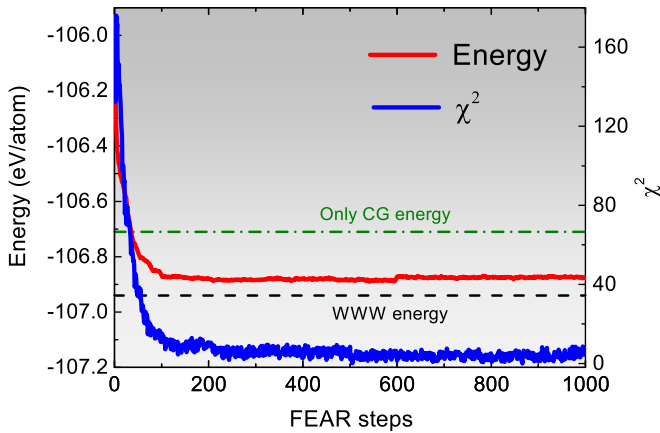


FIG. 6. Total energy per atom and χ^2 vs FEAR steps for a 216-atom *a*-Si model. The green and black broken lines represent the energy per atom for the CG-only and WWW model, respectively.

the first few hundred steps with a simultaneous decrease of E and χ^2 . We then reach a period of “saturation” in which there are tiny fluctuations in the energy and χ^2 . This indicates that the system has reached a region of the energy landscape of *a*-Si, which is characterized by configurations having more or less the same average energy with some disordered fluctuations. We have reported a particular “snapshot” of a conformation, and we discussed it above. However, many conformations in the saturated part of the plot are equally meaningful. Fortunately, they do not fluctuate much, reflecting the fact that the experimental data and the chemistry converge to a well-defined collection of configurations. We track the fluctuations of the average coordination number in Fig. 7, excised from the last 500 steps of FEAR. For convenience, we also show the results for a simulation using the pair-correlation data from a WWW model as reported in Ref. [9]. The use

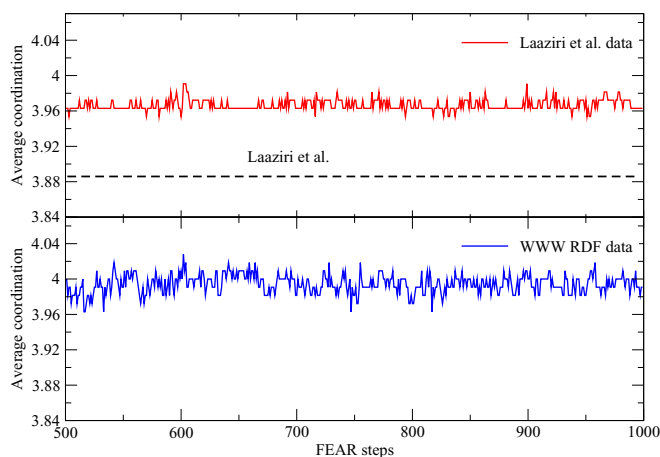


FIG. 7. Variation of the average coordination number for the final 500 steps of FEAR using two different input RDF data. The upper panel is for high-energy x-ray diffraction data from Laaziri *et al.* [14], and the lower panel is for the WWW radial distribution function (RDF) as input data [9]. The broken horizontal line in the upper panel represents the average coordination number, 3.88, reported by Laaziri *et al.* [14].

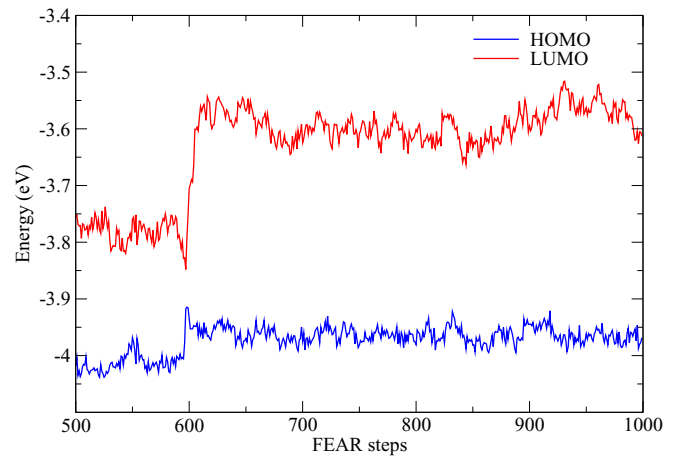


FIG. 8. Variation of the highest occupied molecular orbital (HOMO) level and the lowest unoccupied molecular orbital (LUMO) level for the final 500 steps of FEAR. Note the annihilation of an electronic (gap state) defect near 600 steps.

of WWW pair correlation, as input “experimental” data, forces the network to have fewer defects compared to the real experimental data. This has been reflected in the average coordination number of the FEAR models obtained by using experimental pair-correlation and WWW pair-correlation data. The former produces a FEAR model with an average coordination of 3.96, whereas the latter leads to an average value of 3.99.

In Fig. 8, we also track the fluctuations in the electronic gap for the last 500 steps of FEAR, as crudely estimated as the energy splitting between the LUMO and HOMO levels. It is of considerable interest that, for the last 500 FEAR steps, there is a substantial variation in the electronic density of states near the Fermi level, even though the FEAR process had already reached a “steady state” value for χ^2 and total energy (cf. Fig. 6). Observe too that, while the HOMO level is fairly stationary, the LUMO meanders with relative impunity as it does not contribute to the total energy, being above the Fermi level [42]. Thus, we see that FEAR effectively generates an ensemble of candidate structural models for *a*-Si, which are essentially indistinguishable according to χ^2 and energy. Nevertheless, this affords another opportunity to use *a priori* information—we should select one of these models with the gap most like the experimental sample. To our knowledge, the electronic density of states is not well characterized for the sample, but if it was it would be natural to use it as an additional criterion to select the most experimentally realistic FEAR model. In effect, if we had electronic information, it would break the “structural degeneracy” emphasizing the information-based nature of our approach.

It is evident from Fig. 6 that the FEAR model has a lower energy than its CG-only counterpart. Table I lists the total energy per atom with respect to the energy of the WWW model, which is set at 0.0 eV for convenience. The energy for the FEAR model is found to be 0.06 eV/at, which is approximately 33% lower than the CG-only model with a total energy of 0.09 eV/at. This is a reasonable number compared with other published work [43].

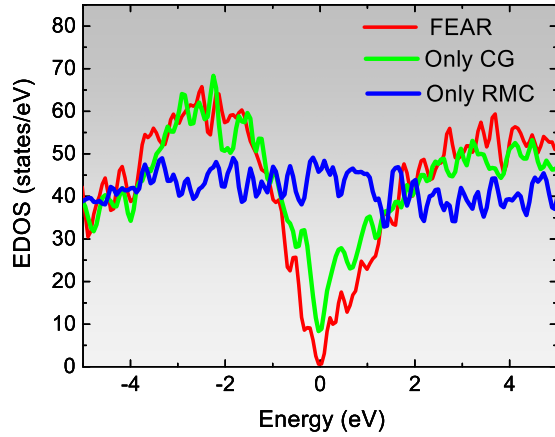


FIG. 9. Electronic density of states (EDOS) of *a*-Si obtained from FEAR (red), CG-only (green), and pure RMC (blue) models. The Fermi levels are located at 0 eV.

The electronic density of states (EDOS) of *a*-Si obtained from the FEAR, CG-only, and RMC models is shown in Fig. 9. For the 216-atom FEAR model, the quality of the EDOS is significantly improved compared with that of the CG-relaxed model and the RMC model. The latter is completely featureless, and it does not provide any useful electronic information. A significant number of defect states clutters the gap in the FEAR model, which is a prediction in this case, since the EDOS has not, to our knowledge, been measured for the annealed sample whose pair correlation data we have employed in our work. Electronic localization is studied using the inverse participation ratio (IPR) [44], which is shown in Fig. 10. The IPR measures the localization of electronic states. For a completely localized state, the IPR value is unity, reflecting that the state is localized around a single atomic site. A completely delocalized or extended state, on the other hand, is distributed over N atoms or sites producing the value of $1/N$. In the FEAR model, the electronic gap is filled by several extended defect states, whereas the WWW model has a clean electronic gap with localized tail states in the vicinity

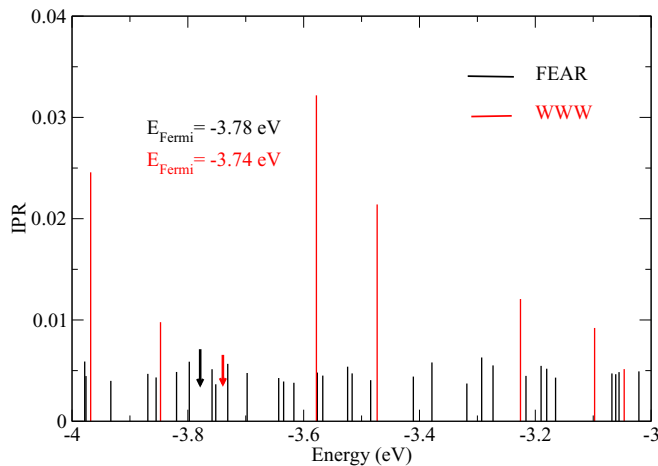


FIG. 10. Inverse participation ratio (IPR) of a 216-atom *a*-Si model for FEAR (black) and RMC (red) models near the gap. Fermi levels are shown by arrows of respective colors.

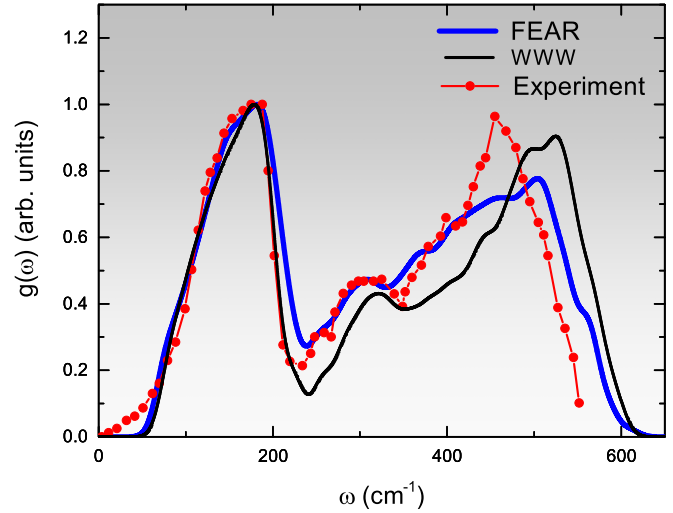


FIG. 11. Vibrational density of states of *a*-Si, $g(\omega)$, from a 216-atom FEAR model (blue) and a WWW model (black). The experimental data (red) shown here are from Kamitakahara *et al.* [47].

of the band edges. In the case of the FEAR model, banding or coupling among the states in the gap leads to an expected delocalization [45] and is reflected in the corresponding IPR values.

The vibrational density of states (VDOS) is computed by estimating the force-constant matrix from finite-difference calculations resulting from perturbing the atoms of a well-relaxed 216-atom FEAR model by 0.02 \AA in six directions ($\pm x$, $\pm y$, and $\pm z$ axes), and calculating the forces on all the remaining atoms for each perturbed configuration. The eigenvalues and eigenvectors are obtained by diagonalizing the dynamical matrix, the details of which can be found in a recent work by Bhattacharai and Drabold [46]. The VDOS for the 216-atom FEAR model is shown in Fig. 11. The computed VDOS is in rather good agreement with the experimental VDOS obtained from inelastic neutron scattering experiments [47]. The exception, probably a shortcoming of our Hamiltonian, is a shift in the high-frequency optical tail by $\sim 35 \text{ cm}^{-1}$. A similar observation applies for the VDOS from WWW model (cf. Fig. 11). This is consistent with the results obtained from other empirical and *ab initio* molecular-dynamics simulations [48,49]. We also note that wavelengths larger than our supercell size L are not included in the computed VDOS, which is reflected in the VDOS by the presence of size artifacts below $k \sim \frac{2\pi}{L}$.

The specific heat in the harmonic approximation can be readily obtained from the vibrational density of states $g(\omega)$. We compute the specific heat $C_v(T)$ using the relation [50,51]

$$C_v(T) = 3R \int_0^{E_{\max}} \left(\frac{E}{k_B T} \right)^2 \frac{e^{E/k_B T}}{(e^{E/k_B T} - 1)^2} g(E) dE, \quad (1)$$

where $g(E)$ is normalized to unity.

Figure 12 shows the dependence of the specific heat on temperature by plotting $\frac{C_v}{T}$ versus T at low temperature from 5 to 300 K for the FEAR model. The inset in Fig. 12 indicates the classical limit, $C_v \approx 3R$, at high temperature. The results show that $C_v(T)$ for the FEAR model are in good agreement

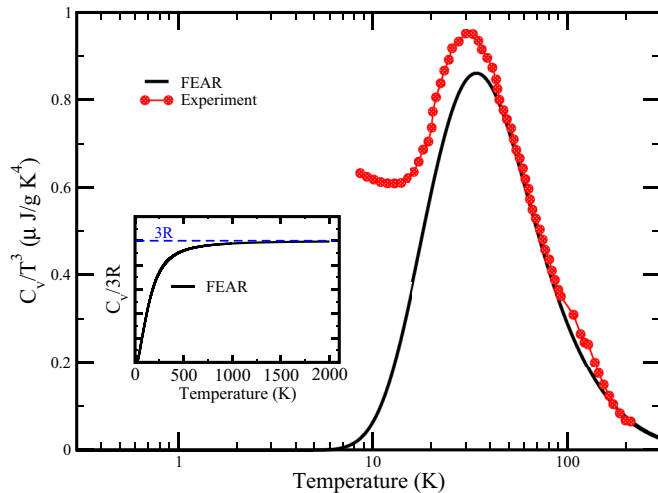


FIG. 12. The specific-heat capacity (C_V/T^3) for a 216-atom a -Si FEAR model (black) compared to the experiment [52]. The inset shows the classical “Dulong-Petit” limit at higher temperature.

with the experimental data from Ref. [52] for $T > 40$ K. This is an additional indication that the FEAR model is correctly reproducing features of a -Si beside those “built in” (from the experimental pair-correlation data), and it is also an indication of consistency between very different physical observables.

IV. CONCLUSIONS

In this paper, we have studied a -Si using an approach called FEAR. The experimental structure factor of a -Si [14] has been employed in FEAR along with *ab initio* interactions to generate a homogeneous model consistent with the data and at a plausible energy minimum according to reliable interatomic interactions. FEAR retains the simplicity and logic of RMC and successfully augments it with a total-energy functional and forces to generate structures that are energetically stable, even exhibiting a satisfactory VDOS. The method

can also be viewed as a way to undertake first-principles modeling of materials when structural experiments are available.

By using an entirely information-based approach, educated by chemistry through the CG subloops, we find highly plausible models derived from experimental data with interesting similarities to and differences from continuous random network models. Following this logic, the best that we can hope to achieve is a structural model jointly agreeing with all experiments, but critically augmented with chemical information in an unbiased mode, as we offer here.

To conclude, this paper offers a method that is genuinely effective for the best known difficult structural inversion problem in the physics of amorphous materials (the structure of a -Si). A method that works well here is likely to have broad applicability (and indeed, we are building up the proof of that statement in ongoing research as we publish this, in addition to the work reported in Refs. [8,9]). We observe that the method is immediately applicable to glasses and amorphous materials of *any kind*, including (perhaps) systems such as amorphous pharmaceuticals. Already the approach has been applied successfully with plane-wave density-functional theory to amorphous GeSeAg systems and amorphous phases of silica and silicon. While no method is ever perfect, this paper demonstrates the need to explore this line of inquiry for the general structural inversion problem.

ACKNOWLEDGMENTS

We thank the U.S. NSF for supporting this work under Grants No. DMR 150683, No. 1507166, and No. 1507670, and the Ohio Supercomputer Center for computer time. We acknowledge the financial support of the Condensed Matter and Surface Science program of Ohio University. We particularly thank Sjoerd Roorda for sharing his diffraction data, which formed the basis for this paper. We further thank Normand Mousseau for helpful suggestions.

-
- [1] V. Ramakrishnan, *Angew. Chem. Int. Ed.* **49**, 4355 (2010).
 - [2] P. Biswas, R. Atta-Fynn, and D. A. Drabold, *Phys. Rev. B* **69**, 195207 (2004).
 - [3] O. Gereben and L. Pusztai, *Phys. Rev. B* **50**, 14136 (1994).
 - [4] R. L. McGreevy and L. Pusztai, *Mol. Sim.* **1**, 359 (1988).
 - [5] R. L. McGreevy, *J. Phys.: Condens. Matter* **13**, R877 (2001).
 - [6] E. T. Jaynes, *Phys. Rev.* **106**, 620 (1957).
 - [7] T. Proffen and S. J. L. Billinge, *J. Appl. Crystallogr.* **32**, 572 (1999).
 - [8] A. Pandey, P. Biswas, and D. A. Drabold, *Phys. Rev. B* **92**, 155205 (2015).
 - [9] A. Pandey, P. Biswas, and D. A. Drabold, *Sci. Rep.* **6**, 33731 (2016).
 - [10] R. A. Street, *Hydrogenated Amorphous Silicon* (Cambridge University Press, Cambridge, 2005).
 - [11] I. Santos, L. A. Marques, L. Pelaz, and L. Colombo, *Phys. Rev. B* **83**, 153201 (2011).
 - [12] Y. Pan, F. Inam, M. Zhang, and D. A. Drabold, *Phys. Rev. Lett.* **100**, 206403 (2008).
 - [13] G. T. Barkema and N. Mousseau, *Phys. Rev. Lett.* **77**, 4358 (1996).
 - [14] K. Laaziri, S. Kycia, S. Roorda, M. Chicoine, J. L. Robertson, J. Wang, and S. C. Moss, *Phys. Rev. Lett.* **82**, 3460 (1999).
 - [15] A. Pandey, B. Cai, N. Podraza, and D. A. Drabold, *Phys. Rev. Appl.* **2**, 054005 (2014).
 - [16] P. Dagenais, J. L. Laurent, and S. Roorda, *J. Phys.: Condens. Matter* **27**, 295801 (2015).
 - [17] D. Beeman, R. Tsu, and M. F. Thorpe, *Phys. Rev. B* **32**, 874 (1985).
 - [18] F. Wooten, K. Winer, and D. Weaire, *Phys. Rev. Lett.* **54**, 1392 (1985).
 - [19] D. N. Tafen and D. A. Drabold, *Phys. Rev. B* **71**, 054206 (2005).
 - [20] M. J. Cliffe, M. T. Dove, D. A. Drabold, and A. L. Goodwin, *Phys. Rev. Lett.* **104**, 125501 (2010).
 - [21] M. J. Cliffe *et al.*, [arXiv:1609.00668](https://arxiv.org/abs/1609.00668).

- [22] K. Prasai, P. Biswas, and D. A. Drabold, *Sci. Rep.* **5**, 15522 (2015).
- [23] K. Prasai, P. Biswas, and D. A. Drabold, *Phys. Status Solidi A* **213**, 1653 (2016).
- [24] G. Opletal, T. C. Petersen, D. G. McCulloch, I. K. Snook, and I. Yarovsky, *J. Phys.: Condens. Matter* **17**, 2605 (2005).
- [25] O. Gereben and L. Pusztai, *J. Comput. Chem.* **33**, 2285 (2012).
- [26] A. K. Soper, *Mol. Phys.* **99**, 1503 (2001).
- [27] P. Biswas, D. N. Tafen, R. Atta-Fynn, and D. Drabold, *J. Phys.: Condens. Matter* **16**, S5173 (2004).
- [28] P. Biswas, D. N. Tafen, F. Inam, B. Cai, and D. A. Drabold, *J. Phys.: Condens. Matter* **21**, 084207 (2009).
- [29] A. Pandey and D. A. Drabold (unpublished).
- [30] D. A. Drabold, Y. Li, B. Cai, and M. Zhang, *Phys. Rev. B* **83**, 045201 (2011).
- [31] M. M. J. Treacy and K. B. Borisenko, *Science* **335**, 950 (2012).
- [32] R. Timilsina and P. Biswas, *J. Phys.: Condens. Matter* **25**, 165801 (2013).
- [33] P. Biswas and R. Timilsina, *J. Phys.: Condens. Matter* **23**, 065801 (2011).
- [34] P. Biswas and S. R. Elliott, *J. Phys.: Condens. Matter* **27**, 435201 (2015).
- [35] P. Biswas, D. A. Drabold, and R. Atta-Fynn, *J. Appl. Phys.* **116**, 244305 (2014).
- [36] N. Nosengo, *Nature (London)* **533**, 22 (2016).
- [37] M. G. Tucker, D. A. Keen, M. T. Dove, A. L. Goodwin, and Q. Hui, *J. Phys.: Condens. Matter* **19**, 335218 (2007).
- [38] J. M. Soler *et al.*, *J. Phys.: Condens. Matter* **14**, 2745 (2002).
- [39] Assuming that the bond-angle distribution in *a*-Si can be approximated by a Gaussian or normal distribution $N(\theta, \sigma)$, the half-width at half-maximum (Γ_{HWHM}) of the distribution can be expressed as $\Gamma_{\text{HWHM}} \approx 1.18\sigma$.
- [40] P. Keblinski, M. Z. Bazant, R. K. Dash, and M. M. Treacy, *Phys. Rev. B* **66**, 064104 (2002).
- [41] M. Ishimaru, S. Munetoh, and T. Motooka, *Phys. Rev. B* **56**, 15133 (1997).
- [42] K. Prasai, P. Biswas, and D. A. Drabold, *Semicond. Sci. Technol.* **31**, 073002 (2016).
- [43] D. A. Drabold, *Phys. Status Solidi RRL* **5**, 359 (2011).
- [44] J. J. Ludlam, S. N. Taraskin, S. R. Elliott, and D. A. Drabold, *J. Phys.: Cond. Matter* **17**, L321 (2005).
- [45] J. Dong and D. A. Drabold, *Phys. Rev. Lett.* **80**, 1928 (1998).
- [46] B. Bhattacharai and D. A. Drabold, *J. Non-Cryst. Solids* **439**, 6 (2016).
- [47] W. A. Kamitakahara, C. M. Soukoulis, H. R. Shanks, U. Buchenau, and G. S. Grest, *Phys. Rev. B* **36**, 6539 (1987).
- [48] S. M. Nakhmanson and D. A. Drabold, *J. Non-Cryst. Solids* **266-269**, 156 (2000).
- [49] A. Valladares, R. M. Valladares, F. Alvarez-Ramírez, and A. A. Valladares, *J. Non-Cryst. Solids* **352**, 1032 (2006).
- [50] A. A. Maradudin, *Theory of Lattice Dynamics in the Harmonic Approximation* (Academic, New York, 1963).
- [51] S. M. Nakhmanson and D. A. Drabold, *Phys. Rev. B* **58**, 15325 (1998).
- [52] B. L. Zink, R. Pietri, and F. Hellman, *Phys. Rev. Lett.* **96**, 055902 (2006).